

# Low-impact development (LID) control feasibility in a small-scale urban catchment for altered climate change scenarios


Abhinav Wadhwa, Venkatesh Budamala, Pavan Kumar Kummamuru, K. S. Kasiviswanathan & Srimuruganandam B

**To cite this article:** Abhinav Wadhwa, Venkatesh Budamala, Pavan Kumar Kummamuru, K. S. Kasiviswanathan & Srimuruganandam B (2023) Low-impact development (LID) control feasibility in a small-scale urban catchment for altered climate change scenarios, Hydrological Sciences Journal, 68:13, 1881-1894, DOI: [10.1080/02626667.2023.2239797](https://doi.org/10.1080/02626667.2023.2239797)

**To link to this article:** <https://doi.org/10.1080/02626667.2023.2239797>

 View supplementary material [↗](#)


---

 Published online: 21 Aug 2023.

---

 Submit your article to this journal [↗](#)

---

 Article views: 123

---

 View related articles [↗](#)

---

 View Crossmark data [↗](#)

---

# Low-impact development (LID) control feasibility in a small-scale urban catchment for altered climate change scenarios

Abhinav Wadhwa<sup>a</sup>, Venkatesh Budamala<sup>a</sup>, Pavan Kumar Kummamuru<sup>b,c</sup>, K. S. Kasiviswanathan<sup>b</sup> and Srimuruganandam B<sup>d</sup>

<sup>a</sup>Interdisciplinary Centre for Water Research (ICWaR), Indian Institute of Science (IISc), Bengaluru, India; <sup>b</sup>Department of Water Resources Development and Management, Indian Institute of Technology (IIT) Roorkee, Roorkee, India; <sup>c</sup>Department of Civil Engineering, Vasavi College of Engineering, Hyderabad, India; <sup>d</sup>Centre for Clean Environment (CCE), Vellore Institute of Technology, Vellore, India

## ABSTRACT

Rainfall is considered a major input in designing stormwater management measures, especially for any low-impact development (LID) control design. With the impact of climate change, rainfall frequency and its patterns are changing continuously. Quantification of these changes and their impact on the performance of LID design becomes crucial. This paper presents a methodology to quantify the change in rainfall patterns using the Coupled Model Intercomparison Project 5 (CMIP5) climate model and to select the most feasible LID for a catchment with haphazard development. Interconnected decentralization-based LID controls are evaluated with the objective of emulating a pre-urbanized scenario. The overall analyses indicated that green roof (GR) followed by infiltration trenches (IT), rooftop disconnection (RTD), and permeable pavement (PP) showed better performance. Furthermore, a combination of IT, PP, and RTD accomplishes better efficiency for extreme rainfall events. Implementation of the most feasible combination will provide the additional benefit of water recycle and reuse.

## ARTICLE HISTORY

Received 20 March 2023  
Accepted 20 June 2023

## EDITOR

A. Castellarin

## ASSOCIATE EDITOR

E. Davies

## KEYWORDS

urban stormwater management; LID controls; climate change; rainfall disaggregation; SWMM

## 1 Introduction

The continuous quantification and prediction of surface runoff generated in urban catchments is a complex task due to uncertain rainfall patterns, haphazard development, and disturbance of the natural hydrological processes. The dynamics of hydrological processes rapidly alter as a result of the difficulty in distinguishing the explicit behaviour of haphazard development and urban sprawl. While haphazard land-use changes with urbanization continue to exert an influence, climate change contributes additional complexity to the regional hydrological cycle, and subsequently leads to a great challenge in devising appropriate mitigation measures.

Various stormwater control measures exist, such as water sensitive urban design (WSUD) (Australia); low impact development (LID)/green infrastructure (GI) (United States); sustainable urban drainage systems (SuDS) (United Kingdom); decentralized rainwater/stormwater management (DRWM) (Germany); sound water cycle on national planning (SWCNP) (Japan); smart water city (SWC), U-eco city (South Korea), best management practices (BMPs) (India), and low impact urban design and development (LIUDD) (New Zealand) (Fletcher *et al.* 2015, Che and Zhang 2019), hereafter referred to as the LID controls for this study. Implementation of LIDs emulates pre-urban hydrological characteristics by reducing the peak runoff, increasing the infiltration potential, and reducing the time to peak for events. Processes such as infiltration, storage, evaporation, pollutant

treatment, and storage of runoff near its source are controlled by LIDs (AL-Hamati *et al.* 2010, Wang *et al.* 2021). The selection of any LID for an urban parcel is evaluated based on its efficacy to reduce, recycle, and reuse the excess surface runoff passing through impervious areas (Jiang and McBean 2021, Zhu *et al.* 2021).

Oliazadeh *et al.* (2021) summarized studies demonstrating the selection and implementation of various LIDs to mitigate surface runoff and increase infiltration potential. Wadhwa and Pavan Kumar (2020) performed a study on an urban catchment by implementing the eight major LIDs. On a performance basis, LIDs are categorized into three types: storage type, by-pass type, and a combination of these. The study concluded that the performance of storage-based management measures is effective in reducing peak runoff, increasing infiltration potential, and increasing storage efficiency. Several studies performed cost–benefit analyses to provide recommendations to urban planners in selecting the most economical LID (Coffman *et al.* 2000, 2004, Allen *et al.* 2010, Islam *et al.* 2011, Lee *et al.* 2012, Risch *et al.* 2015, Brudler *et al.* 2016, Jeong *et al.* 2016, Marchi *et al.* 2016, Bahrami *et al.* 2019, Shrivastava and Unnikrishnan 2019, Nguyen *et al.* 2020). The effectiveness of LID controls was studied and the research outcomes indicated that net expected benefits are achieved from the reusability of impervious runoff harvested through LIDs (Liu *et al.* 2016, Marchi *et al.* 2016, da Silva *et al.* 2018, Bhatt *et al.* 2019, Jiang and McBean 2021, Wang *et al.* 2021, Zhang *et al.* 2021a, 2021b).

Climate change suggests that the design of stormwater management measures computed using runoff generated from historical rainfall data will tend to create problems in the future (Haddad *et al.* 2009, Akbari-Alashti *et al.* 2014, Bertrand-Krajewski 2020). Apart from the potential impacts of climate change and land-use change on the performance of LIDs, the location of LIDs plays a crucial role. The general practice is to construct LIDs at flooding nodes, typically located in the downstream section of a catchment (Wadhwa and Pavan Kumar 2020). To identify the flooding nodes, it is essential to check the catchment's behaviour in various extreme rainfall events. Fine-scale data is required to simulate the catchment for long-term scenarios.

Most urban parcels in developing countries such as India lack the availability of well-laid raingauge stations, and it becomes difficult to measure continuous minute-wise climatic data (Burns *et al.* 2012, De Paola *et al.* 2015, Gyasi-Agyei and Mahbub 2007, Jung *et al.* 2015, Licznar *et al.* 2011, Loganathan and Mahindrakar 2021, Müller and Haberlandt 2018, Sun *et al.* 2019). Hence, for this purpose, satellite data is often downscaled to the required regional level. Recent advances have shown a peculiar development in the downscaling of data. For instance, Schaller *et al.* (2020) demonstrated the challenges of higher spatial and temporal resolution in simulating flood impacts. Liu *et al.* (2020) proposed a rainfall downscaling algorithm to address the problem of deficiency in rainfall data at the desired scale during flash flood events in any hydrologic/hydraulic simulation. Apparently, it is essential to curtail the error between finer and coarser resolution rainfall data engendered using any downscaling algorithm. To do so, various disaggregation methods are continuously used to convert data at a daily scale to the hourly or sub-hourly scale (Mendes and Marengo 2010, Lee and Jeong 2014, McIntyre *et al.* 2016, Loganathan and Mahindrakar 2020, Schaller *et al.* 2020, Pan *et al.* 2021). Among various methodologies of downscaling, regression-based downscaling has received limited attention although it provides better approximation power. The daily rainfall data is downscaled to minute-wise data following the methods described by AL-Areeq *et al.* (2021), Barbaro *et al.* (2021), Scher and Peßenteiner (2021), and Lee and Hsu (2021).

To solve the issues of quantification of extreme rainfall events and attenuate their impact on catchments, an integrated flood model is developed in this study using the Stormwater Management Model (SWMM). Adaptive Emulator Modelling-based Optimization – Genetic Algorithm (AEMO-GA) is applied to generate near real-time fine-resolution data using a mechanism to validate with the observed data. An application of the proposed methodology at Vellore Institute of Technology (VIT) is demonstrated in this study. To identify the location of LID measures, an intensive location-based study is carried out which sequentially supports the selection and stimulation of LIDs for an urban or semi-urban catchment. This location-based study relies on land availability for construction, slope, distance, stream order, soil structure, capital investment, and minimal hindrance. To assess LID feasibility for long-term benefits, downscaled climatic data using AEMO-GA are employed in the subsequent simulations. A ranking-based algorithm based on the performance of LIDs is used to identify the most suitable combination that can be adopted to emulate the pre-urban scenario.

## 2 Study area description

A highly developed and well-planned catchment in VIT, an educational institute located at latitude 12.95°N and longitude 79.19°E, in the town of Vellore, Tamil Nadu, India, was chosen to demonstrate the methodology proposed in this paper. The pre-development (corresponding to the year 1995) and post-development (corresponding to the year 2021) land use details of the study area are shown in Fig. 1(a) and (b). The major changes in the built-up area are represented in red. In the year 1995, the percentage of imperviousness was about 23%, whereas in 2021 imperviousness had increased to 62%. The major features of the campus comprise roads, buildings (academic and non-academic), playgrounds, parking lots, and open space for greenery; among these, the prominent features are roads and buildings. Out of the total campus area of 372 ha, impervious types of land uses such as buildings and roads occupy about 207.36 ha (i.e. about 62% of the total).

The campus has a well-laid open rectangular storm sewer network that carries runoff from adjoining roads and other impervious areas. The storm sewer network of the campus was first planned to be laid out during the year 1995 and subsequent additions were made to the network in succeeding years as more and more impervious features were added in the campus. The runoff from these sewer lines is discharged to an artificial lake (with a surface area of about 4 ha) in the campus vicinity. The presently existing storm sewer network was completed in the year 2010 and has not changed since that time, although there has been a drastic increase in the impervious area within the past decade. Rooftop rainwater harvesting is diligently practised throughout the campus such that the rainfall from the building rooftops is discharged either to the groundwater system or to the storm sewer network, from which the water discharges into the lake. The lake is used only for aesthetic purposes and not to meet potable or non-potable water demands. Apart from rooftop rainwater harvesting, a green roof has been installed at the Technology Tower building, and in the near future this may be extended to other buildings.

## 3 Methodology

A detailed flowchart describing the proposed methodology for selecting the most feasible LID control is presented in Fig. 2. The methodology is divided into three sections: (1) identification of top-ranked climate models; (2) generating an Intensity-Duration-Frequency (IDF) curve using statistical downscaling of climate model and GA-based disaggregation algorithms; (3) observing the performance of LID controls under top-ranked climate models and ranking the most suitable LID control option. For any flash flood event, the stormwater generated is for a short duration and the performance of LID control during this interval needs to be critically analysed. The first step in this study was to identify the best-suited climate model specific to the study area. Following the procedure described in Jeganathan and Andimuthu (2013), three best-suited climate models were selected. The data were downscaled and disaggregated to 15-minute intervals using the K-fold regression technique and GA optimization. In the next step, a standard multivariate regression technique was used to develop IDF curves corresponding to disaggregated rainfall data for the study area. These IDF curves formed the basis to identify the

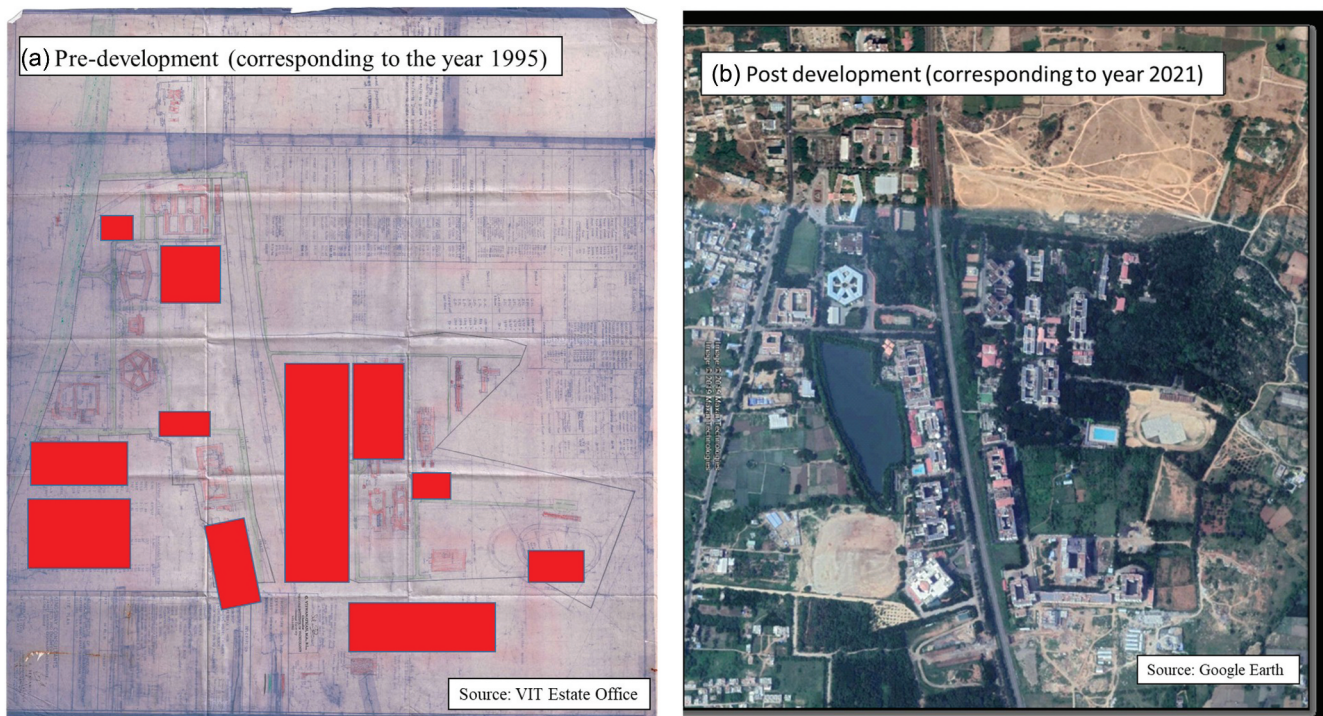


**Figure 1.** Study area: (a) Proposed layout of VIT campus in the year 1995; (b) VIT campus in the year 2020 with an increase in urbanization of 62% (major changes in build-up are shown in red).

performance of LID controls evaluated using SWMM for a highly urbanized catchment. Finally, out of all the LID controls the most feasible LID control measure is identified and recommended for stormwater management.

### 3.1 Identification of best-suited climate model

The precipitation and temperature for the study area of Vellore, Tamil Nadu, were extracted from the Coupled Model Intercomparison Project 5 (CMIP5) datasets. A total of 10 models are found suitable for the Tamil Nadu region of India, for a daily ensemble realization run (r1i1p1): Australian Community Climate and Earth System Simulator (ACCESS), Community Climate System Model 4 (CCSM4), Canadian coupled ocean-atmosphere general circulation model 4 (CanCM4), Canadian Earth System Model 2 (CanESM2), European community Earth System Model (EC-EARTH), Geophysical Fluid Dynamics Laboratory Coupled Model (GFDL-CM3), Meteorological Research Institute Coupled Global Climate Model Version Three (MRI-CGM3), Max Planck Institute Earth System Model Low Resolution (MPI-ESM-LR), Norwegian Climate Center's Earth System Model (NorESM1-M), and REgional MOdel 2015 (REMO2015) (Jeganathan and Andimuthu 2013). The daily precipitation and temperature data pertaining to the study area for the past 70 years (1950 to 2020) were obtained from the India Meteorological Department (IMD) repository (<http://mausam.imd.gov.in>). The output of each climate model was compared with the data from IMD using statistical evaluation indices such as normalized root mean square error (NRMSE), percentage bias (PBIAS), Nash-Sutcliffe efficiency (NSE), RMSE-observations standard deviation (RSR), entropy and correlation

(CORR) (Jeganathan and Andimuthu 2013, Das and Umamahesh 2016, Loganathan and Mahindrakar 2020).

### 3.2 Generating IDF curve equations for the best-suited climate model

The annual maximum data series is prepared for different rainfall durations. Gumbel's extreme value Type I distribution (Chow *et al.* 1988, Majumdar and Gupta 2009, Fu and Butler 2014) is the most commonly used probability density function for analysing hydrological extremes.

In this paper, the IDF equations were derived for the three best-ranked climate models with various scenarios, i.e. Representative Concentration Pathways (RCP)4.5 and RCP8.5. For this purpose, the daily rainfall data of each climate model was disaggregated to intervals of 15 minutes, 30 minutes, 1 hour, 2 hours, 6 hours, and 12 hours using a GA-optimization algorithm based on the K-nearest neighbour (KNN) classifier technique. Downscaling derives the data from a coarser time step to a finer time step. Different approaches were developed to downscale the data but they are limited to precipitation downscaling. However, the present study focused on global downscaling by introducing the AEMO-GA strategy (lower-fidelity physically-based surrogate methodology) for different variables which derives from coarser to finer resolution. The lower-fidelity AEMO evaluates the trends of the neighbourhood points and later downscales the data using GA. Here, the adaptive technology was applied to the tuning of emulator models. Finally, the temporally downscaled data of the gauge sub-basin were transferred to each ungauged sub-basin through aggregated weights.

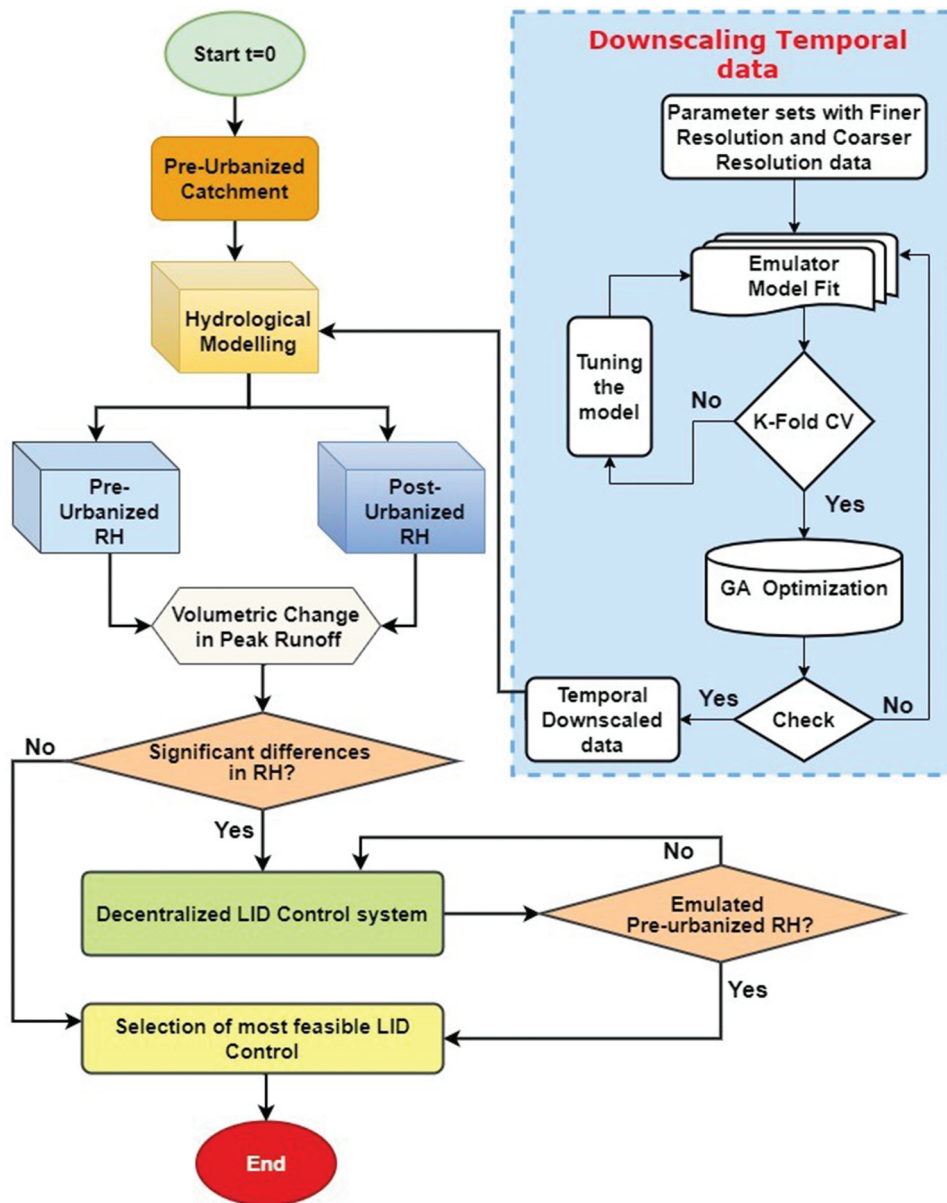


Figure 2. Flowchart describing the proposed methodology.

### 3.3 Performance of LID controls under selected climate models

The selection of the most feasible LID or a combination of LIDs was simulated using SWMM. SWMM is a widely used open-source package for planning, modelling, and managing sustainable drainage and urban stormwater management. It simulates stormwater and sanitary sewer flows including treatment in typical LIDs. SWMM is a distributed, dynamic rainfall–runoff simulation model used for a single event or long-term simulation of runoff quantity and quality from primarily urban areas. SWMM uses the momentum equation (i.e. the St Venant equation) and the continuity equation to model the flow through the storm sewers.

Apart from modelling flow through storm sewers (referred to as conduits in the SWMM interface), SWMM is also capable of modelling pollutant load from urban areas and checking the suitability of various stormwater BMPs (e.g. LID, SuDS, WSUD) for urban stormwater management. SWMM software

allows the user to easily apply various control measures to manage the peak runoff generated through a single sub-catchment section. SWMM comes with an in-built function of different types of LID controls. A summary of each of the LID controls available in SWMM is given in Table 1. For this study, each of the LID controls was applied to the case study area and was evaluated for pre-defined performance measures (peak reduction, storage efficiency, and infiltration potential). A total of eight LID control options were tested in the case study area: bio-retention tanks (BR), rain garden (RG), green roof (GR), infiltration trench (IT), permeable pavement (PP), rain barrel (RB), rooftop disconnection (RTD), and vegetative swales (VS).

GR has been partially implemented in one of the buildings on the VIT campus (the Technological Tower building) with vegetation growth adopted across the open spaces in corridors (Wadhwa and Pavan Kumar 2020). The details of various input data parameters used for the analysis and the design of different LID options in SWMM are shown in Table 1. The optimal size of an

**Table 1.** Layer-wise LID controls parameters and the area available for their construction.

SCM Parameters		Units	BR	RG	GR	IT	PP	RB	RTD	VS	IT-PP-RTD
		% Area	6.54	5.32	19.44	7.78	16.42	4.57	7.23	12.39	25.45
Surface	Berm height	mm	400	150	30	150	20	800	500	200	
	Vegetation volume fraction	-	0.1	0.1	0.75	-	-	-	-	0.9	0.75
	Surface roughness	-	0.12	0.12	0.13	0.24	0.014	-	0.014	0.12	0.014
	Surface slope	%	0.1	0.3	1	0.1	1	-	1	0.8	10
Soil	Thickness	mm	500	500	100	-	150	-	-	-	300
	Porosity	-	0.5	0.3	0.5	-	0.5	-	-	-	0.5
	Field capacity	-	0.35	0.2	0.2	-	0.1	-	-	-	0.2
	Wilting point	-	0.187	0.1	0.024	-	0.024	-	-	-	0.1
	Conductivity	mm/h	10	10	30	-	100	-	-	-	10 – 50
	Suction head	mm	210	3.5	60	-	3.5	-	-	-	60 – 100
Storage	Thickness	mm	150	0	-	600	150	-	-	-	400
	Void ratio	-	0.5	0.75	-	0.75	0.4	-	-	-	0.5
	Seepage rate	mm/h	12	20	-	24	1.2	-	-	-	1.2 – 10
	Clogging factor	-	-	0	-	0	-	-	-	-	-
Drain	Barrel height	mm	-	-	-	-	-	-	-	-	-
	Flow coefficient	-	-	-	-	0.69	-	0.68	-	-	0.68
	Flow exponent	-	0.5	-	-	0.5	0.5	0.5	-	-	0.5
	Offset height	mm	6	-	-	6	6	12	-	-	10
Pavement	Thickness	mm	-	-	-	-	100	-	-	-	100
	Void ratio	-	-	-	-	-	0.25	-	-	-	0.25
	Impervious surface fraction	-	-	-	-	-	-	-	-	-	-
	Permeability	mm/h	-	-	-	-	250	-	-	-	250

individual LID option was determined for a storm event with a five-year return period and a rainfall duration of six hours. The performance analysis of different LIDs was carried out using daily rainfall data obtained from selected climate models. The performance efficiency of the LID corresponding to the selected daily rainfall data was determined using the efficiency measures described by Sorup *et al.* (2016) and Wadhwa and Pavan Kumar (2020), which are as follows:

- (1) **Volumetric efficiency ( $E_{fp}$ ):** The ratio of the annual volume of water contained by the LIDs ( $V_{managed}$ ) to the total annual inflow to the LIDs from impervious areas ( $V_{Annual\ inflow}$ ). Mathematically, this is expressed as:

$$E_{fp} = \frac{V_{managed}}{V_{Annual\ inflow}} \tag{1}$$

- (1) **Runoff efficiency ( $E_{rr}$ ):** The recurrence interval of the peak storm event for any LID plays an important role in identifying the type of LID adopted in an urbanized or non-urbanized catchment. The runoff efficiency indirectly relates to the performance of LIDs in reducing the

peak runoff from the catchment. Mathematically, it is expressed as:

$$E_{rr} = \frac{V_{Runoff\ reduced}}{V_{Annual\ inflow}} \tag{2}$$

- (1) **Storage efficiency ( $E_{storage}$ ):** The prime objective of LID in an urbanized area is to manage the peak runoff by accommodating managed water in the form of infiltration or storage tanks. Storage efficiency helps to identify the amount of water that is stored by a particular LID ( $V_{water\ storage}$ ) concerning the total annual inflow to the LID and is expressed as:

$$E_{storage} = \frac{V_{water\ storage}}{V_{Annual\ inflow}} \tag{3}$$

## 4 Results and discussion

### 4.1 Selection of top-ranked climate model

The details of the 10 climate models used for the preliminary analysis are shown in Table 2. The climatic variables from

**Table 2.** General details of climate models and their selection criteria based on ranks obtained.

S.no.	Climate model ID	Origin	Resolution (Lat × Lon)	Latitude (km)	Longitude (km)	Rank for each of the statistical parameter						Total	Final Rank
						NRMSE (1)	PBIAS (2)	RSR (3)	CORR (4)	Entropy (5)	NSE (6)		
1	ACCESS	CSIRO-BOM, Australia	1.9 × 1.2	210	130	6	6	6	5	6	6	29	6
2	CCSM4	NCAR, USA	1.2 × 0.9	130	100	3	2	2	1	3	2	13	1
3	CanCM4	CCCMA, Canada	2.8 × 2.8	310	310	8	7	7	7	7	7	43	8
4	CanESM2	CCCMA, Canada	2.8 × 2.8	310	310	10	10	10	8	10	9	57	10
5	EC-EARTH	EC-Earth, Europe	1.1 × 1.1	120	120	9	9	9	6	9	10	52	9
6	GFDL-CM3	NOAA, GFDA, USA	2.5 × 2.0	275	220	1	1	3	9	1	3	18	3
7	MRI-CGM3	MRI, Japan	1.1 × 1.1	120	120	2	3	4	10	4	4	27	5
8	MPI-ESM-LR	MPI-N, Germany	1.9 × 1.9	210	210	4	4	1	3	2	1	15	2
9	NorESM1-M	NCC, Norway	2.5 × 1.9	275	210	7	8	8	4	8	8	43	8
10	REMO2015	German Weather Service (DWD)	0.22 × 0.22	25	25	5	5	5	2	5	5	27	5

these models were downscaled to a regional scale using the bicubic spline interpolation technique. To downscale each climate model to a regional scale, we followed the methodology adopted by Loganathan and Mahindrakar (2020). Observed data from IMD (1959 to 2020) and VIT (2016 to 2020) weather stations were collected to check the ability of the climate models, which reproduce climatic variables more closely with observed data. Historical data for each climate model is compared with the observed data. The performance of each climate model was analysed using the following statistical parameters: NRMSE, PBIAS, RSR, CORR, entropy, and NSE (Jeganathan and Andimuthu 2013). The climate model yielding the lowest total score was considered most suitable for the region, and the one with the largest total score is considered the least preferred climate model. The ranks of each of the statistical measures obtained for the comparison are shown in Table 2 (columns 7 to 12). The ranks are summed and the final rank is obtained (shown in column 14 of Table 2). The best three climate models for the study area region were found to be (in descending order) CCSM4, MPI-ESM-LR, and GFDL-CM3.

#### 4.2 Downscaling and disaggregating the selected climate models

After the selection of the best GCMs, disaggregation of climate data for the emission scenarios RCP4.5 and RCP8.5 was carried out. Here, RCP4.5 represents the median conditions and RCP8.5 signifies the extreme scenarios of varying future climatic conditions. In this study, rainfall data were generated for the two RCP scenarios under the three GCMs for time intervals of 15 minutes, 30 minutes, 1 hour, 3 hours, 6 hours, and 12 hours. Here, the validation of temporally downscaled data for

a peak rainy-day precipitation value is represented using the polar plot for different time scales (3, 6, 9, 12, 15, 18, 21, and 24 h) with their rainfall ranging from 10 to 70 mm in a day (Fig. 3). The polar plot shows that the variation for the rainfall mostly occurs from 9pm to 3am, wherein the plot shows dense values during this period and scattered values are observed to be unprecedented events. Hence, for both scenarios (RCP4.5 and RCP8.5) for all the climate models, the potential rainfall is expected to happen from 9pm to 6am, and the same is observed in real-time scenarios. Also, the 15-minute hydrograph was validated for high-intensity, medium-intensity, and low-intensity rainfall events. Based on the historical precipitation data, precipitation depths of 14, 3 and 0.25 mm were considered high, medium and low peaks, respectively. In Fig. 3, the peak precipitation for different levels is validated with observed data and provides optimal results in every aspect. Figure 4 shows the maximum possibility of precipitation in every 15-minute interval for both RCP scenarios (4.5 and 8.5). From Fig. 4, it can be observed that the precipitation is greater between 12am and 6am for both moderate and extreme conditions. These variations in the rainfall patterns show that most of the rainfall in the Vellore region happens during the evenings or early mornings. Heavy rainfall events during these periods hinder traffic movement during peak mobility hours, and thus need to be addressed effectively. The most widely used technique to identify the quantity of peak rainfall events is IDF curves corresponding to a specific return period.

#### 4.3 Generation of IDF curves

The daily precipitation data during a period of 33 years (2018 to 2050) for the selected climate models – CCSM4 (CSIRO-

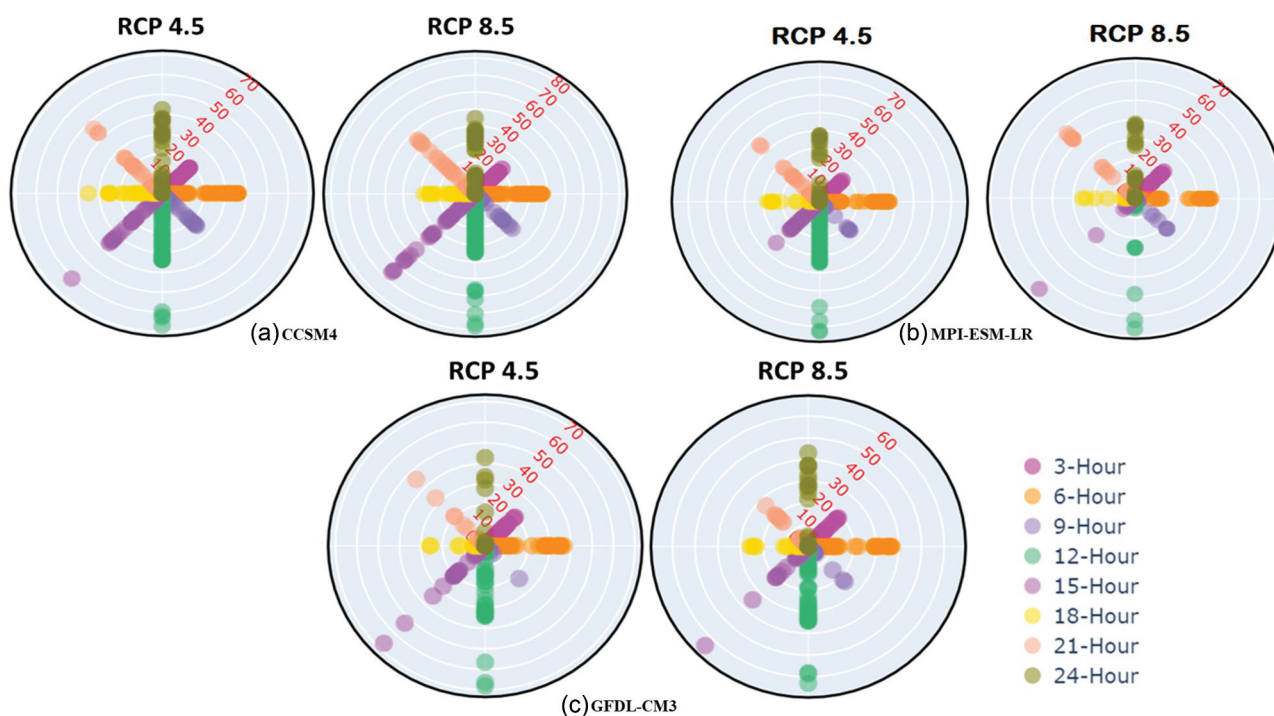


**Figure 3.** Performance evaluation of rainfall disaggregation model for the downscaled data – polar plots for selected RCP scenarios of climate models: (a) CCSM4, (b) MPI-ESM-LR, and (c) GFDL-CM3.

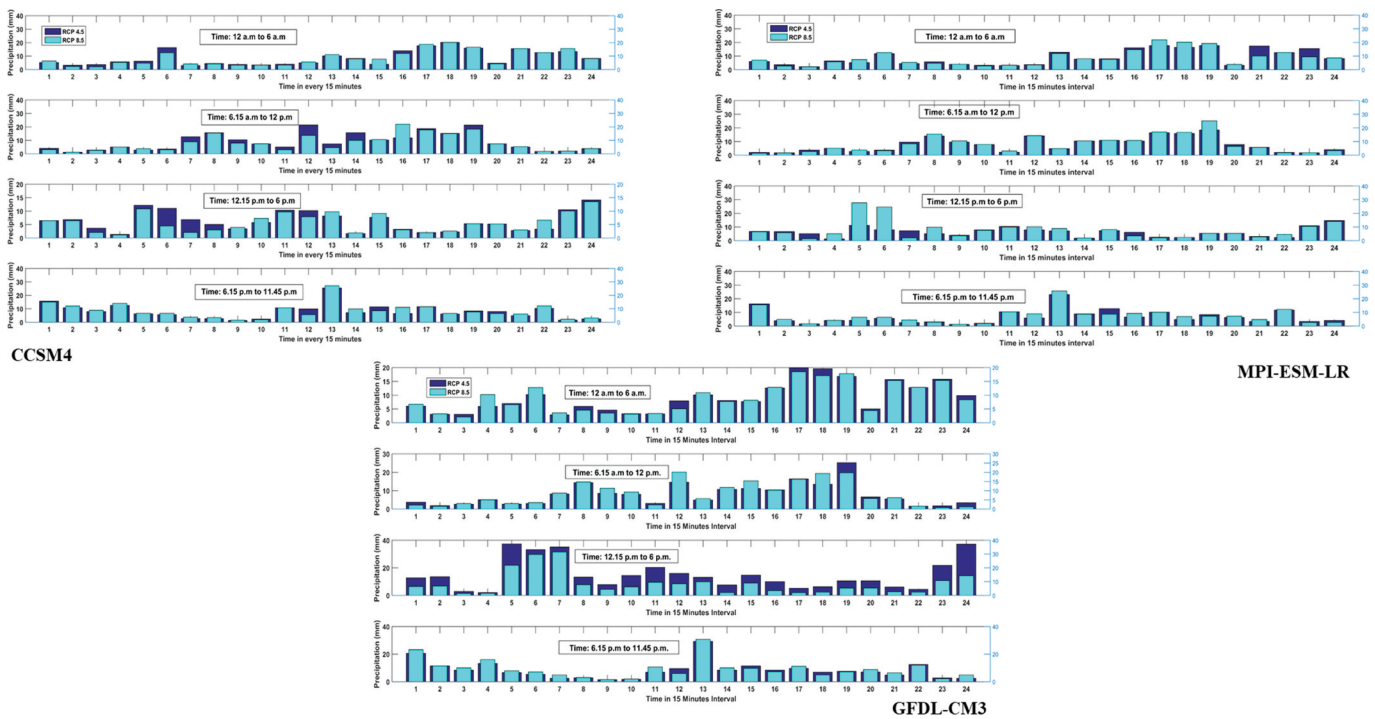


Figure 4. Disaggregation of maximum precipitation event from 30 years of daily data from climate models.

BOM, Australia), MPI-ESM-LR (MPI-N, Germany), and GFDL-CM3 (NOAA-GFDA, USA) – were taken from the respective country agencies. First, the maximum rainfall intensity series was developed for each climate model. Next, the exceedance probability curves of rainfall were developed for each climate model and are shown in the Supplementary material (Fig. S1). The reduced variate and frequency factor values for different return periods for the predicted rainfall data of 33 years (the year 2018 to the year 2050) are shown in Table 3.

To show the effect of climate change on extreme rainfall intensities, the IDF curves of the selected climate models were plotted against the IDF curves of historical rainfall data. The patterns for Gumbel’s extreme value exceedance probability curves for each climate model are consistent with respect to theoretical maximum values (Fig. S1). The comparison curves for different return periods can be seen in the Supplementary material (Figs S2–S4). The IDF curves under the climate models

GFDL-CM3-RCP4.5 and GFDL-CM3-RCP8.5 closely match the historical rainfall data for all return periods. Whereas the IDF curves under climate models MPI-ESM-LR-RCP4.5 and MPI-ESM-LR-RCP8.5 show the greatest deviation from the historical rainfall data for all the return periods. For CCSM4 models, the difference in rainfall intensities for the same duration is greater for higher return periods. The IDF curves thus generated for different climate models are further utilized to test the effectiveness of stormwater control structures in absorbing runoff from impervious areas under different rainfall patterns. It is often more convenient to express IDF curves in the form of an equation so that it becomes easier to determine the design rainfall intensity of the desired return period and for any given duration. In Table 4, the regression equation for each climate model showed an increase in rainfall intensity. While the main focus of this study was to assess the performance of LID controls, a comprehensive evaluation of the IDF curve variation under climate change should be included.

Table 3. Values of the reduced variate  $y_T$  and corresponding frequency factor  $K_T$  for different return periods.

T	2	5	10	25	50	100
$y_T$	0.367	1.5	2.25	3.199	3.902	4.6
$K_T (n = 33)$	-0.153	0.856	1.524	2.369	2.995	3.617

Table 4. IDF equations for different climate models.

Model	Emission scenario	Chi-square	Chi-square error
CCSM4	RCP4.5	$i = \frac{10.387^{0.118}}{(t+0.75)^{1.33}}$	0.046
	RCP8.5	$i = \frac{9.097^{0.22}}{(t+0.84)^{1.43}}$	0.056
MPI-ESM-LR	RCP4.5	$i = \frac{9.077^{0.181}}{(t+0.93)^{1.38}}$	0.062
	RCP8.5	$i = \frac{9.327^{0.159}}{(t+0.89)^{1.37}}$	0.059
GFDL-CM3	RCP4.5	$i = \frac{8.997^{0.192}}{(t+0.95)^{1.38}}$	0.064
	RCP8.5	$i = \frac{10.517^{0.121}}{(t+0.76)^{1.32}}$	0.047



#### 4.4 Location of LIDs

A decentralized arrangement (i.e. a particular LID control unit for a specific landuse feature) for LID controls is considered for the study area. The dimensions of each layer in LID controls as shown in Table 1 were given as input to each LID control. LIDs are located in the catchment in such a way that each building consists of RTD on the rooftop, and a storage type LID in its periphery. The water will flow from the building area to the storage type LID control with time, and the overflow from those LIDs is allowed to flow to the next available LID control through the storm drains. Figure 5(a) and (b) respectively demonstrate a case of no LID control and IT as a LID control implemented in the study area. Junction nodes in the catchment show the location of IT with the storm drain network capacity, mentioned as link capacity, in the study

area. As shown in Fig. 5(a), the nodes have reached their maximum capacity and the flow is travelling through the drains to the next available node which changes the channel flow holding capacity. Most of the nodes were observed to be flooded for high rainfall events, and after the installation of LID controls, flow through the channels is reduced (as shown in Fig. 5(b)) which consequently reduces the peak runoff in the system.

#### 4.5 Performance of LID controls

The performance of LID controls was tested under three different return period scenarios, i.e. day-to-day scenario (0.2-year return period), design scenario (5-year return period), and extreme event scenario (75-year return period).

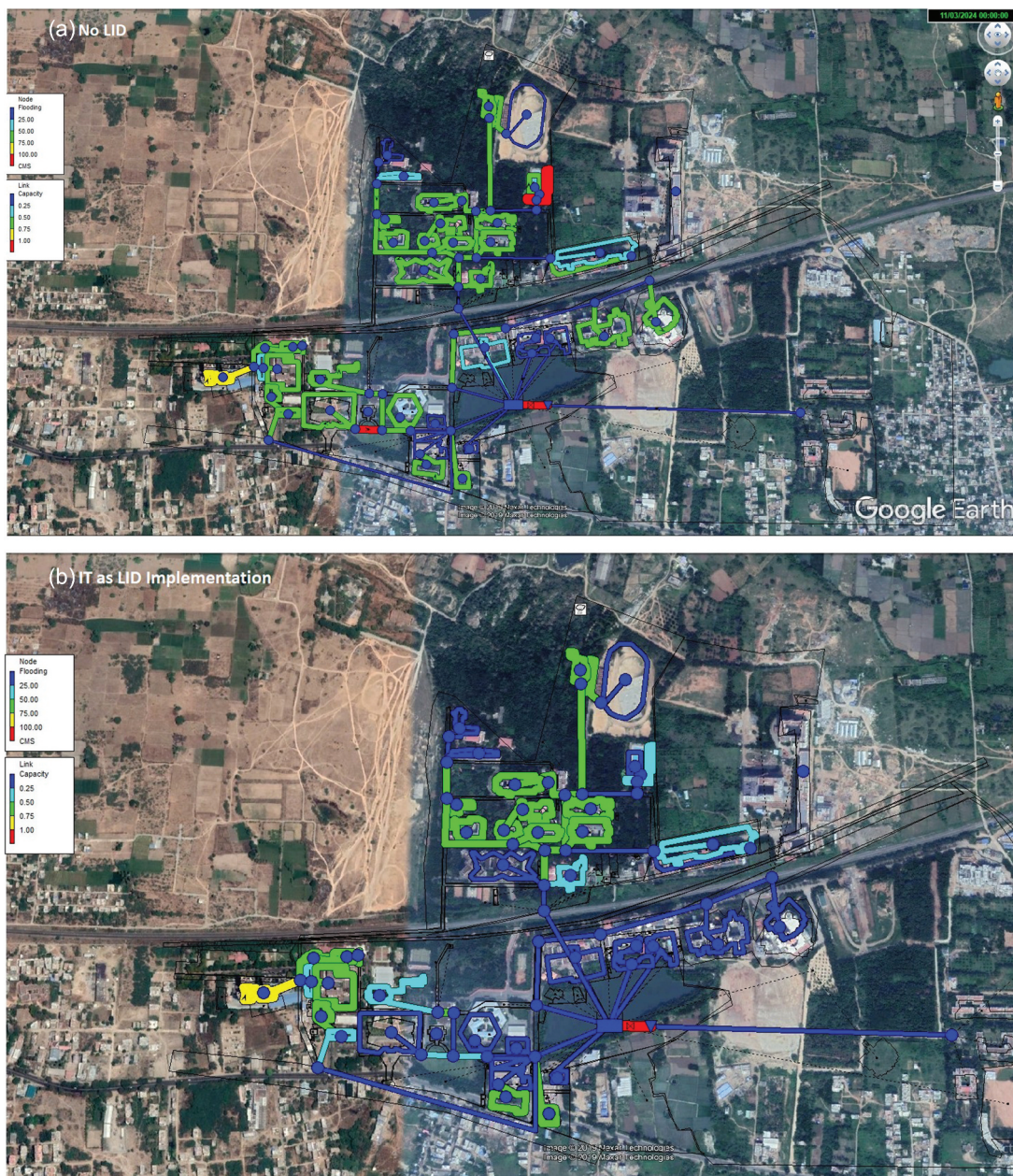


Figure 5. Flow characteristics (a) with no LID implementation; (b) with the implementation of LID such as infiltration trench (IT).

A storm event with a duration of 6 hours with a 15-minute time step was adopted in SWMM with other climatological and topographical inputs. Individually the LID controls were placed in the space available across the building with necessary flow conduits. LID controls are interconnected with conduits having sizes as mentioned in Wadhwa and Pavan Kumar (2020). Other input parameters such as percentage imperviousness, Manning's coefficient, inlet and outlet structures, LID control layer properties, available LIDs in the area, and so on are obtained from Wadhwa and Pavan Kumar (2020) (further modified for the year 2021). The SWMM run was performed for each LID control to identify its maximum potential to reduce peak runoff, increase infiltration potential and enhance the storage potential of the area.

The results corresponding to the percentage reduction in runoff ( $E_{rr}$ ), increase in infiltration potential ( $E_{fp}$ ), and storage efficiency ( $E_{storage}$ ) are shown in Table 5. For each climate model, the top three performing LID controls are selected and shown in Table 6. To identify the most suitable control unit, the LID controls were evaluated on five broad criteria: area availability, runoff peak reduction, aesthetics, and local interaction, increasing infiltration potential, and storage efficiency. The best three LID control measures under each climate change scenario and for different return periods are shown in Table 6. Based on the rank order among various LID control measures shown in Table 5, the following was observed:

- (a) When area availability for construction of LID control is limited: For any highly urbanized catchment, it becomes difficult to identify the overland space to construct the LID controls. In this study, the preference of LID is followed as  $RB > RTD > RG > BR$ .
- (b) When the major priority is to be given to reducing the peak runoff event irrespective of area required or human interaction, the order followed for LID control selection is:  $GR > IT > VS > RTD$ .
- (c) When the major focus is to increase the infiltration potential to emulate the pre-urbanized infiltration potential, this order of LID placement can be followed:  $RG > GR > VS > RTD > PP$ .
- (d) When aesthetics and local interaction are also a major part of LID design and placement: The general perception of the local population is to adopt the LID control measure in which the water is not stored for a long period and the maintenance course is minimal. For this constraint, it becomes crucial for decision makers to provide minimal options to the local populace in order to select the best option. From the analyses performed in this study, out of the eight available LID controls, controls for local population perception can be narrowed down to four (RTD, PP, RB, GR, and VS). Out of these four measures the order of LID placement is:  $PP > GR > RTD > VS > RB$ .
- (e) When the objective is simply to store water for future needs, the order for LID control that can be followed is:  $PP > RB > GR > IT$ .

In the above propositions, ">" means "is better than." It should be noted that even though the GR measure gives the highest

efficiency in many aspects, it is not viable to adopt because of its various limitations (Wadhwa and Pavan Kumar 2020). Also, for most of the climate change scenarios, the performance of IT, PP, and RTD was found to be better overall compared to the other LIDs.

#### 4.6 Daily run scenarios

Apart from the comparison based on the extreme rainfall events generated by IDF curves, the LID controls are subjected to a daily run for the projected 40 years of temperature and rainfall data. Downscaled daily rainfall and temperature data for the climate model and their scenarios were given as an input in SWMM and the annual runoff hydrographs and infiltration curves were developed. In all the selected LID controls, the peak runoff is reduced, and the infiltration potential and storage capacity of the entire catchment increase compared to the no-LID control scenario. Hence, the application of any LID measure will help to reduce the peak intensity, increase the infiltration potential of the area, and increase the storage capacity of the area for further use. The daily run for the catchment showed that implementation of GR on the buildings will help to emulate the pre-urban scenario of the year 2003. But due to the limitations of GR (dead load increase, restrictions to further development, and regular maintenance), it becomes infeasible to apply GR in a full-scale manner. Other LID controls, in the order of their ranking as mentioned in Table 5, showed a substantial reduction in peak flows and a considerable increase in infiltration and storage values. From the hydrographs, the control measures IT, PP, and RTD perform the best to reduce the peak runoff event. From the infiltration curves, it can be concluded that IT, BR, and RG are the best-suited control measures for increasing the infiltration potential of the area.

The most feasible LID control measure is selected by performance ranking with the four selection parameters mentioned in Table 6. From the analysis, it is observed that the combination of IT, PP, and RTD fulfils most of the selection criteria. To demonstrate the variation in surface runoff and infiltration potential of the LID, Figs 6 and 7 are plotted for the annual sum of runoff and infiltration depths. It can be observed that there has been a substantial amount of reduction in runoff and a substantial increase in infiltration for the LID scenario of IT-PP-RTD. Taking water sustainability into consideration, the proposed scenario IT-PP-RTD can be understood as the most feasible solution in a highly developed catchment like the VIT campus.

## 5 Conclusions

The key focus of the study is to determine the most feasible LID control that can provide benefits with both low and extreme flow events, using a simple ranking method based on an overall score using efficiency measures. For this purpose, the LID controls available in the SWMM interface were placed in the study area in a decentralized manner. To identify the locations of LID controls in the campus area, a manual survey was done and empty spaces were identified. The best-suited climate models and their representative concentration pathway scenarios were identified using a simple ranking algorithm

**Table 5.** Improvement of percentage efficiency of each LID control under the climate change conditions for three events: day-to-day (0.2 years), design (5 years), and extreme (75 years).

LID type	$E_{max}$ (%)			$E_p$ (%)			$E_{storage}$ (%)			$E_{max}$ (%)			$E_p$ (%)			$E_{storage}$ (%)		
	0.2 year	5 year	75 year	0.2 year	5 year	75 year	0.2 year	5 year	75 year	0.2 year	5 year	75 year	0.2 year	5 year	75 year	0.2 year	5 year	75 year
CCSM4 RCP4.5																		
IT	23	26	29	29	31	32	22	28	34	18	25	31	26	30	33	24	29	37
GR	29	32	38	32	33	36	16	20	25	36	40	43	35	37	39	21	30	43
BR	15	20	25	34	36	39	10	14	16	11	19	28	32	36	40	10	20	25
PP	18	25	34	29	33	37	34	35	38	28	33	35	24	38	38	42	53	61
RB	15	18	19	18	19	20	23	34	43	13	17	20	17	19	20	23	47	68
RG	18	22	27	39	41	44	15	21	26	13	20	29	37	40	45	15	29	44
RTD	23	17	30	20	22	24	16	17	18	19	26	32	18	22	25	22	25	29
VS	22	26	31	33	35	38	10	15	17	17	24	33	31	34	39	11	20	27
CCSM RCP8.5																		
MPI-ESM-LR RCP4.5																		
IT	19	24	29	27	30	32	24	26	34	19	25	29	27	30	32	22	30	38
GR	36	40	42	35	37	38	21	27	37	37	40	42	36	37	38	19	25	33
BR	11	17	24	32	35	38	10	17	23	12	18	24	32	35	38	10	16	21
PP	28	32	40	24	26	35	42	52	56	29	35	39	25	35	31	41	47	51
RB	13	16	19	17	18	20	24	41	65	13	17	19	17	19	20	23	29	38
RG	14	19	26	37	40	43	15	26	38	15	20	25	38	40	43	15	24	34
RTD	19	25	30	18	21	24	21	24	27	20	25	29	19	21	23	20	22	24
VS	17	23	30	31	34	37	11	18	25	18	24	30	31	34	37	11	17	23
MPI-ESM-LR RCP8.5																		
GFDL-CM3 RCP4.5																		
IT	21	25	29	28	30	32	21	23	30	19	25	30	27	30	33	21	29	35
GR	36	40	42	35	37	38	21	28	39	39	41	43	37	38	39	16	20	25
BR	13	19	25	33	35	38	10	18	25	12	19	26	32	35	39	10	14	16
PP	13	19	32	27	29	36	42	54	59	29	32	38	24	36	34	33	35	38
RB	14	17	19	17	19	20	24	43	68	13	17	20	17	19	20	23	34	43
RG	16	21	27	38	40	43	15	27	40	14	20	27	37	40	44	15	21	26
RTD	21	26	30	19	22	24	12	25	28	20	26	31	18	21	24	16	17	18
VS	20	25	31	32	34	37	11	19	26	18	24	32	31	34	38	10	15	21
GFDL-CM3 RCP8.5																		

**Table 6.** Order of preference of the top three LID controls under different climate models.

Order no.	Day-to-day event	Design event	Extreme event	Order no.	Day-to-day event	Design event	Extreme event	Order no.	Day-to-day event	Design event	Extreme event
CCSM4 RCP4.5				CCSM4 RCP8.5				MPI-ESM-LR RCP4.5			
<b>If runoff reduction is the main priority</b>											
1	GR	GR	GR	1	GR	GR	GR	1	GR	GR	GR
2	IT	IT	PP	2	PP	PP	PP	2	PP	PP	PP
3	RTD	VS	VS	3	RTD	RTD	VS	3	IT	RTD	RTD
<b>If increasing infiltration potential is the main priority</b>											
1	RG	RG	RG	1	RG	RG	RG	1	RG	RG	RG
2	BR	BR	BR	2	GR	PP	BR	2	GR	GR	GR
3	GR	VS	VS	3	VS	GR	VS	3	BR	BR	BR
<b>If increasing storage efficiency is the main priority</b>											
1	PP	PP	RB	1	PP	PP	RB	1	PP	PP	RB
2	RB	RB	PP	2	IT	RB	PP	2	RB	RB	PP
3	IT	IT	IT	3	RB	GR	GR	3	IT	GR	RG
GFDL-CM3 RCP4.5				GFDL-CM3 RCP8.5				MPI-ESM-LR RCP8.5			
1	GR	GR	GR	1	GR	GR	GR	1	GR	GR	GR
2	IT	RTD	PP	2	PP	PP	PP	2	PP	PP	PP
3	RTD	IT	IT	3	RTD	RTD	IT	3	RTD	VS	VS
<b>If increasing infiltration potential is the main priority</b>											
1	RG	RG	RG	1	RG	RG	RG	1	RG	RG	RG
2	GR	GR	GR	2	GR	GR	GR	2	BR	GR	GR
3	BR	BR	BR	3	BR	PP	BR	3	VS	PP	BR
<b>If increasing storage efficiency is the main priority</b>											
1	PP	PP	RB	1	PP	PP	RB	1	PP	PP	PP
2	RB	RB	PP	2	RB	RB	PP	2	RB	IT	IT
3	IT	GR	RG	3	IT	IT	IT	3	RB	RB	RB

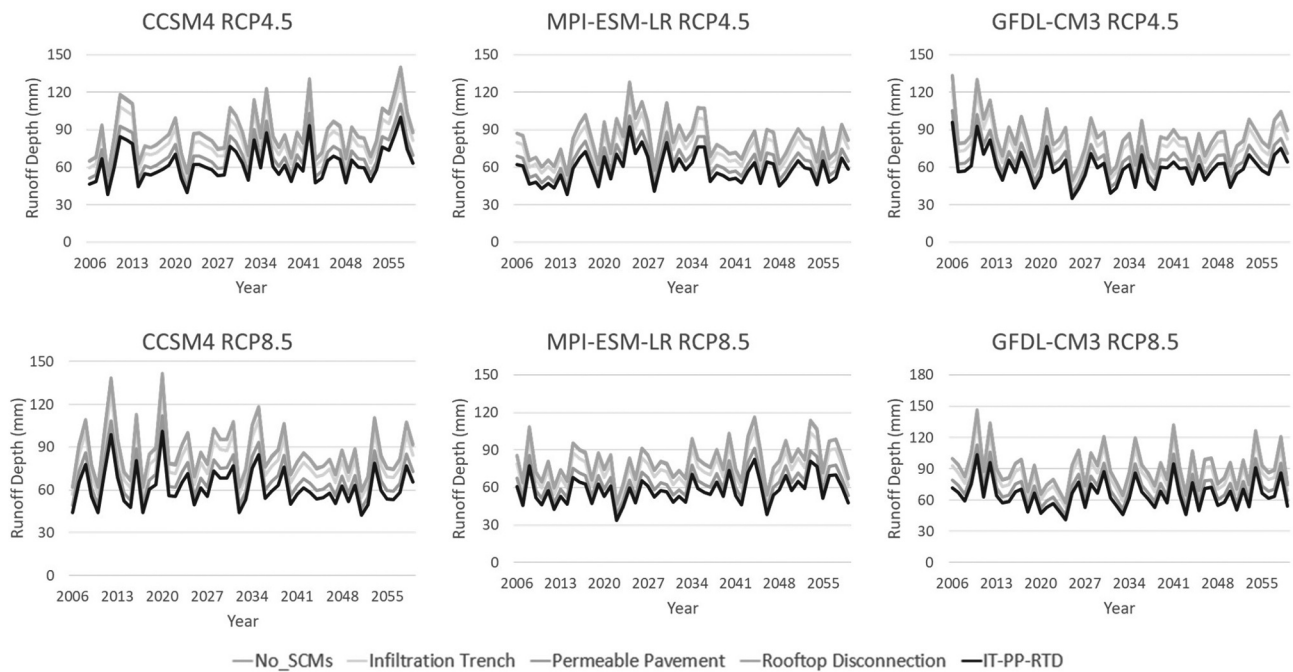


**Figure 6.** Projected annual runoff generation from the top four LIDs against no LID under different climate models.

with respect to observed data. From the results of this ranking algorithm, CCSM4, MPI-ESM-LR, and GFDL-CM3 were found to be the three best-ranked models for the Vellore region. The daily data obtained after down-scaling these models were disaggregated to different time steps (intervals of 15 minutes, 30 minutes, 1 hour, 3 hours, 6 hours, and 12 hours) using the GA-optimization disaggregation technique. The outcomes from the GA-

optimization algorithm for the disaggregated data showed a good correlation with the observed 15-minute data provided by IMD. IDF curves corresponding to these climate models are developed and a storm event of 6 h @ 0.2 years, 6 h @ 5 years, and 6 h @ 75 years with a time step of 15 minutes is generated for evaluating the performance of different LID controls. The efficiency measures adopted to identify the most suitable LID control measure for the

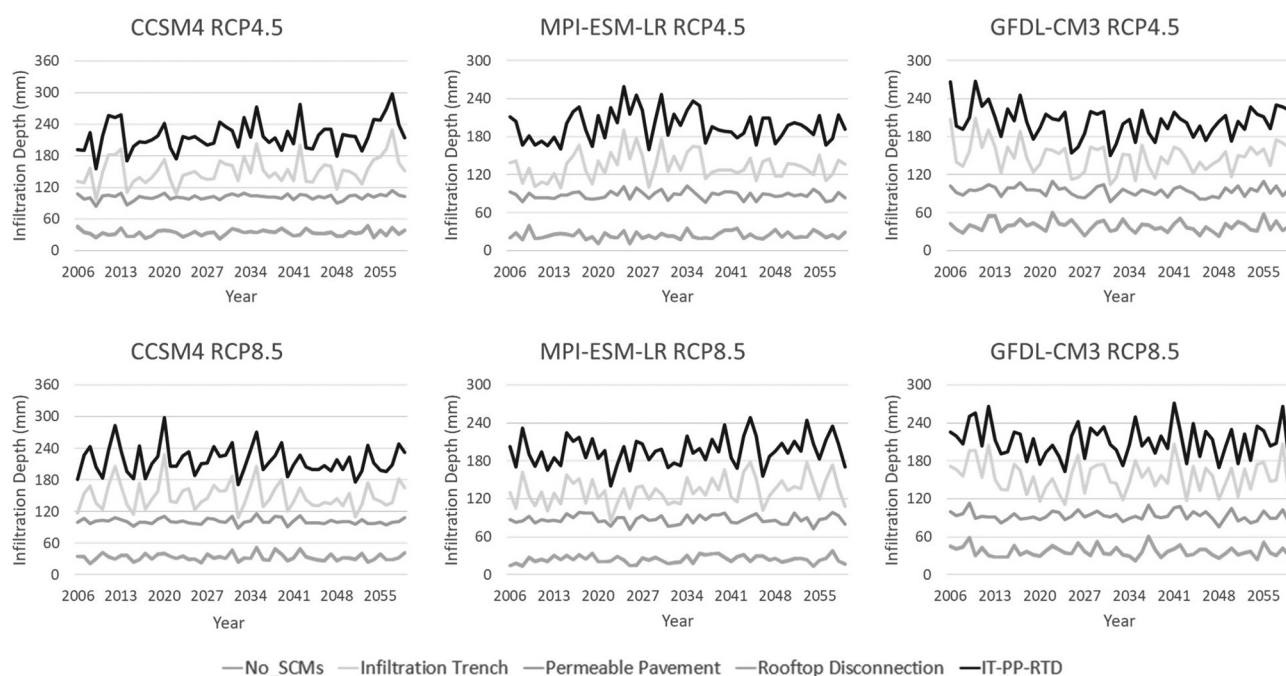


**Figure 7.** Projected annual infiltration curves from the top four LIDs against no LID under different climate model.

study area were: runoff reduction efficiency, infiltration potential efficiency, and storage efficiency. Each LID control measure was evaluated for these efficiency measures and climate models. The results showed that for different events the top three LID controls are roughly similar for each climate model. Leaving aside GR as an alternative, IT, RTD, and PP can be considered the three most feasible LID controls under different climate models.

The combination of these LID controls is further applied to the catchment with daily projected data for each climate model. The runoff hydrographs and infiltration curves thus obtained are compared with the hydrographs and infiltration curves for the no-LID control scenario and other LID control scenarios. From the runoff hydrographs, a substantial reduction (approximately 46%) in the peak runoff is observed in the IT-PP-RTD scenario as compared to the no-LID control scenario. Similarly, the infiltration potential is increased by 41–44% compared to the no-LID scenario. Additionally, the storage capacity of the catchment is increased by 16% compared to the no-LID scenario. This shows that the implementation of the combination of IT, PP, and RTD can be suggested as the most feasible LID measure which will be capable of handling the climate change impacts on the semi-urbanized catchment.

### Acknowledgements

The authors are thankful to IMD, the VIT Estate office and Google Earth for providing various types of support during the completion of the present work. We also acknowledge that there was no funding agency involved in the study and all the data used are open source and freely available on the websites mentioned in the study. Finally, we thank the reviewers and the editor for their profound and constructive comments.

### Disclosure statement

No potential conflict of interest was reported by the authors.

### ORCID

Pavan Kumar Kummamuru  <http://orcid.org/0000-0002-1839-5819>  
 K. S. Kasiviswanathan  <http://orcid.org/0000-0003-4706-6931>  
 Srimuruganandam B  <http://orcid.org/0000-0003-1324-5552>

### Ethics declaration

The authors certify that they have no affiliations with or involvement in any organization or entity with any financial interest or non-financial interest (such as personal or professional relationships) in the subject matter or materials discussed in this article.

### References

- Akbari-Alashti, H., *et al.*, 2014. Multi-reservoir real-time operation rules: a new genetic programming approach. *Proceedings of the Institution of Civil Engineers - Water Management*, 167 (10), 561–576. doi:10.1680/wama.13.00021
- AL-Areeq, A., Al-Zahrani, M., and Chowdhury, S., 2021. Rainfall intensity-duration-frequency (IDF) curves: effects of uncertainty on flood protection and runoff quantification in southwestern Saudi Arabia. *Arabian Journal for Science and Engineering*, 46 (11), 10993–11007. doi:10.1007/s13369-021-06142-0
- AL-Hamati, A.A.N., Ghazali, A.H., and Mohammed, T.A., 2010. Determination of storage volume required in a sub-surface stormwater detention/retention system. *Journal of Hydro-Environment Research*, 4 (1), 47–53. doi:10.1016/j.jher.2009.12.002
- Allen, V., Walker, T., and Schemper, T., 2010. Development and application of modular LID site planning tool. In: *Low impact development of 2010 redefining water city - Proceedings of the 2010 international low impact development conference*. San Francisco, CA, 714–721. doi:10.1061/41099(367)63
- Bahrami, M., Bozorg-Haddad, O., and Loáiciga, H.A., 2019. Optimizing stormwater low-impact development strategies in an urban watershed considering sensitivity and uncertainty. *Environmental Monitoring and Assessment*, 191 (6). doi:10.1007/s10661-019-7488-y
- Barbaro, G., *et al.*, 2021. Innovations in best practices: approaches to managing urban areas and reducing flood risk in reggio calabria (Italy). *Sustainability*, 13 (6). doi:10.3390/su13063463

- Bertrand-Krajewski, J.-L., 2020. Integrated urban stormwater management: evolution and multidisciplinary perspective. *Journal of Hydro-Environment Research*. doi:10.1016/j.jher.2020.11.003
- Bhatt, A., Bradford, A., and Abbassi, B.E., 2019. Cradle-to-grave life cycle assessment (LCA) of low-impact-development (LID) technologies in southern Ontario. *Journal of Environmental Management*, 231, 98–109. doi:10.1016/j.jenvman.2018.10.033
- Brudler, S., et al., 2016. Life cycle assessment of stormwater management in the context of climate change adaptation. *Water Research*, 106, 394–404. doi:10.1016/j.watres.2016.10.024
- Burns, M.J., et al., 2012. Hydrologic shortcomings of conventional urban stormwater management and opportunities for reform. *Landscape and Urban Planning*, 105 (3), 230–240. doi:10.1016/j.landurbplan.2011.12.012
- Che, W. and Zhang, W., 2019. Urban stormwater management and sponge city concept in China. *Urban Water Management for Future Cities: Technical and Institutional Aspects from Chinese and German Perspective*, 3–11. doi:10.1007/978-3-030-01488-9\_1
- Chow, V.T., Maidment, D.R., and Mays, L.W., 1988. Applied hydrology. International association of scientific hydrology. *Bulletin*. doi:10.1080/0262666509493376
- Coffman, L., Clar, M., and Weinstein, N., 2000. Low impact development management strategies for Wet Weather Flow (WWF) control. In: *Building partnerships*. Vol. 104. Reston, VA: American Society of Civil Engineers, 1–7. doi:10.1061/40517(2000)109
- Coffman, L., Clar, M., and Weinstein, N., 2004. Low impact development management strategies for Wet Weather Flow (WWF) control. *Joint conference on water resource engineering and water resources planning and management 2000: Building partnerships*, Vol. 104. Minneapolis, MN. doi:10.1061/40517(2000)109
- da Silva, C.V.F., et al., 2018. Climate change impacts and flood control measures for highly developed urban watersheds. *Water (Switzerland)*, 10 (7), 1–18. doi:10.3390/w10070829
- Das, J. and Umamahesh, N.V., 2016. Downscaling monsoon rainfall over River Godavari Basin under different climate-change scenarios. *Water Resources Management*, 30, 5575–5587. doi:10.1007/s11269-016-1549-6
- De Paola, F., et al., 2015. Sustainable development of storm-water systems in African cities considering climate change. *Procedia Engineering*, 119 (1), 1181–1191. doi:10.1016/j.proeng.2015.08.970
- Fletcher, T.D., et al., 2015. SUDS, LID, BMPs, WSUD and more – the evolution and application of terminology surrounding urban drainage. *Urban Water Journal*, 12 (7), 525–542. doi:10.1080/1573062X.2014.916314
- Fu, G. and Butler, D., 2014. Copula-based frequency analysis of overflow and flooding in urban drainage systems. *Journal of Hydrology*, 510, 49–58. doi:10.1016/j.jhydrol.2013.12.006
- Gyasi-Agyei, Y. and Mahbub, S.M.P.B., 2007. A stochastic model for daily rainfall disaggregation into fine time scale for a large region. *Journal of Hydrology*, 347 (3–4), 358–370. doi:10.1016/j.jhydrol.2007.09.047
- Haddad, O.B., et al., 2009. Optimal cultivation rules in multi-crop irrigation areas. *Irrigation and Drainage*, 58 (1), 38–49. doi:10.1002/ird.381
- Islam, N., et al., 2011. Reviewing source water protection strategies: a conceptual model for water quality assessment. *Environmental Reviews*, 19 (1), 68–105. doi:10.1139/A11-001
- Jeganathan, A. and Andimuthu, R., 2013. Developing climate change scenarios for Tamil Nadu, India using MAGICC/SCENGEN. *Theoretical and Applied Climatology*, 114 (3–4), 705–714. doi:10.1007/s00704-013-0871-7
- Jeong, H., et al., 2016. Life cycle assessment of low impact development technologies combined with conventional centralized water systems for the City of Atlanta, Georgia. *Frontiers of Environmental Science & Engineering*, 10 (6), 1–13. doi:10.1007/s11783-016-0851-0
- Jiang, A.Z. and McBean, E.A., 2021. Performance of lot-level low impact development technologies under historical and climate change scenarios. *Journal of Hydro-Environment Research*, 38, 4–13. doi:10.1016/j.jher.2021.07.004
- Jung, M., et al., 2015. Analysis of effects of climate change on runoff in an urban drainage system: a case study from Seoul, Korea. *Water Science and Technology*, 71 (5), 653–660. doi:10.2166/wst.2014.341
- Lee, J.G., et al., 2012. A watershed-scale design optimization model for stormwater best management practices. *Environmental Modelling & Software*, 37, 6–18. doi:10.1016/j.envsoft.2012.04.011
- Lee, M.-H. and Hsu, I.-P., 2021. Estimation of the annual rainfall erosivity index based on hourly rainfall data in a tropical region. *Soil and Water Research*, 16 (2), 74–84. doi:10.17221/25/2020-SWR
- Lee, T. and Jeong, C., 2014. Nonparametric statistical temporal downscaling of daily precipitation to hourly precipitation and implications for climate change scenarios. *Journal of Hydrology*, 510, 182–196. doi:10.1016/j.jhydrol.2013.12.027
- Licznar, P., Łomotowski, J., and Rupp, D.E., 2011. Random cascade driven rainfall disaggregation for urban hydrology: an evaluation of six models and a new generator. *Atmospheric Research*, 99 (3–4), 563–578. doi:10.1016/j.atmosres.2010.12.014
- Liu, X., et al., 2020. A new framework for rainfall downscaling based on EEMD and an improved fractal interpolation algorithm. *Stochastic Environmental Research and Risk Assessment*, 34 (8), 1147–1173. doi:10.1007/s00477-020-01823-y
- Liu, Y., et al., 2016. Optimal selection and placement of BMPs and LID practices with a rainfall-runoff model. *Environmental Modelling & Software*, 80, 281–296. doi:10.1016/j.envsoft.2016.03.005
- Loganathan, P. and Mahindrakar, A.B., 2020. Assessment and ranking of CMIP5 GCMs performance based on observed statistics over Cauvery river basin – peninsular India. *Arabian Journal of Geosciences*, 13 (22). doi:10.1007/s12517-020-06217-6
- Loganathan, P. and Mahindrakar, A.B., 2021. Statistical downscaling using principal component regression for climate change impact assessment at the Cauvery river basin. *Journal of Water and Climate Change*, 12, 2314–2324. doi:10.2166/wcc.2021.223
- Majumdar, C. and Gupta, G., 2009. Willingness to pay and municipal water pricing in transition: a case study. *Journal of Integrative Environmental Sciences*, 6 (4), 247–260. doi:10.1080/19438150903068224
- Marchi, A., Dandy, G.C., and Maier, H.R., 2016. Integrated approach for optimizing the design of aquifer storage and recovery stormwater harvesting schemes accounting for externalities and climate change. *Journal of Water Resources Planning and Management*, 142 (4), 04016002. doi:10.1061/(ASCE)WR.1943-5452.0000628
- McIntyre, N., Shi, M., and Onof, C., 2016. Incorporating parameter dependencies into temporal downscaling of extreme rainfall using a random cascade approach. *Journal of Hydrology*, 542, 896–912. doi:10.1016/j.jhydrol.2016.09.057
- Mendes, D. and Marengo, J.A., 2010. Temporal downscaling: a comparison between artificial neural network and autocorrelation techniques over the Amazon Basin in present and future climate change scenarios. *Theoretical and Applied Climatology*, 100 (3), 413–421. doi:10.1007/s00704-009-0193-y
- Müller, H. and Haberlandt, U., 2018. Temporal rainfall disaggregation using a multiplicative cascade model for spatial application in urban hydrology. *Journal of Hydrology*, 556, 847–864. doi:10.1016/j.jhydrol.2016.01.031
- Nguyen, T.T., et al., 2020. A new model framework for sponge city implementation: emerging challenges and future developments. *Journal of Environmental Management*, 253 (October 2019), 109689. doi:10.1016/j.jenvman.2019.109689
- Oliazadeh, A., et al., 2021. Developing an urban runoff management model by using satellite precipitation datasets to allocate low impact development systems under climate change conditions. *Theoretical and Applied Climatology*. Springer Vienna. doi:10.1007/s00704-021-03744-4
- Pan, S., et al., 2021. Temporary dependency of parameter sensitivity for different flood types. *Hydrology Research*, 52 (5), 990–1014. doi:10.2166/nh.2021.187
- Risch, E., et al., 2015. Life cycle assessment of urban wastewater systems: quantifying the relative contribution of sewer systems. *Water Research*, 77, 35–48. doi:10.1016/j.watres.2015.03.006
- Schaller, N., et al., 2020. The role of spatial and temporal model resolution in a flood event storyline approach in western Norway. *Weather and Climate Extremes*, 29 (June), 100259. doi:10.1016/j.wace.2020.100259
- Scher, S. and Peßenteiner, S., 2021. Technical note: temporal disaggregation of spatial rainfall fields with generative adversarial networks. *Hydrology and Earth System Sciences*, 25 (6), 3207–3225. doi:10.5194/hess-25-3207-2021

- Shrivastava, S. and Unnikrishnan, S., 2019. Review of life cycle assessment and environmental impacts from the oil & Gas sector. In: G. R. P. J. R. M. Jain K. Sangle S., ed. *Managing technology for inclusive and sustainable growth - 28th international conference for the international association of management*. Excel India Publishers, 972–984. <https://www.scopus.com/inward/record.uri?eid=2-s2.0-85081110534&partnerID=40&md5=446eee38ced3a3e424b193b5ebc81266>
- Sorup, H.J.D., et al., 2016. Efficiency of stormwater control measures for combined sewer retrofitting under varying rain conditions: quantifying the three points approach (3PA). *Environmental Science & Policy*, 63, 19–26. doi:10.1016/j.envsci.2016.05.010
- Sun, Y., et al., 2019. Deriving intensity–duration–frequency (IDF) curves using downscaled in situ rainfall assimilated with remote sensing data. *Geoscience Letters*, 6 (1). doi:10.1186/s40562-019-0147-x
- Wadhwa, A. and Pavan Kumar, K., 2020. Selection of best stormwater management alternative based on storm control measures (SCM) efficiency indices. *Water Policy*, 22 (4), 702–715. doi:10.2166/wp.2020.168
- Wang, J., et al., 2021. Comparison of infiltration models to describe infiltration characteristics of bioretention. *Journal of Hydro-Environment Research*, 38, 35–43. doi:10.1016/j.jher.2021.08.002
- Zhang, W., et al., 2021a. Influence of rainfall on the performance of bioretention systems modified with activated carbon and biochar. *Journal of Hydro-Environment Research*, 38, 63–71. doi:10.1016/j.jher.2021.06.001
- Zhang, Z., et al., 2021b. Improvement of rainwater infiltration and storage capacity by an enhanced seepage well: from laboratory investigation to HYDRUS-2D numerical analysis. *Journal of Hydro-Environment Research*, 39, 15–24. doi:10.1016/j.jher.2021.10.001
- Zhu, D.Z., et al., 2021. Sustainable urban drainage: current interests and future needs. *Journal of Hydro-Environment Research*, 38, 1–3. doi:10.1016/j.jher.2021.09.002